

Time-Resolved Photoelectron Spectroscopy of Dissociating 1,2-Butadiene Molecules by High Harmonic Pulses

Ryo Iikubo,[†] Takehisa Fujiwara,[†] Taro Sekikawa,^{*,†} Yu Harabuchi,[‡] Sota Satoh,[‡] Tetsuya Taketsugu,[‡] and Yosuke Kayanuma[§]

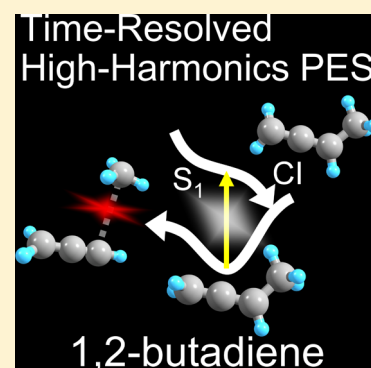
[†]Department of Applied Physics, Faculty of Engineering, Hokkaido University, Kita 13 Nishi 8, Kita-ku, Sapporo 060-8628, Japan

[‡]Department of Chemistry, Faculty of Science, Hokkaido University, Kita 10 Nishi 8, Kita-ku, Sapporo 060-0810, Japan

[§]Materials and Structures Laboratory, Tokyo Institute of Technology, 4259 Nagatsuta, Midori-ku, Yokohama 226-8503, Japan

S Supporting Information

ABSTRACT: Using 42 nm high harmonic pulses, the dissociation dynamics of 1,2-butadiene was investigated by time-resolved photoelectron spectroscopy (TRPES), enabling us to observe dynamical changes of multiple molecular orbitals (MOs) with higher temporal resolution than conventional light sources. Because each lower-lying occupied MO has particular spatial electron distribution, the structural dynamics of photochemical reaction can be revealed. On the femtosecond time scale, a short-lived excited state with a lifetime of 37 ± 15 fs and the coherent oscillation of the photoelectron yield stimulated by Hertzberg-Teller coupling were observed. Ab initio molecular dynamics simulations in the electronically excited state find three relaxation pathways from the vertically excited structure in S_1 to the ground state, and one of them is the dominant relaxation pathway, observed as the short-lived excited state. On the picosecond time scale, the photoelectron yields related to the C–C bond decreased upon photoexcitation, indicating C–C bond cleavage.



One of the most simplified perspectives of photochemical reactions of molecules is the atomic rearrangement accompanying bond breaking and recombination upon photoexcitation. Photoelectron spectroscopy (PES) is advantageous to the investigation of chemical reactions, including biological processes, in that the electrons constituting the chemical bonds are probed directly.^{1–5} PES measures the ionization energies, which are correlated with the molecular orbital (MO) energies under the Koopmans' theorem.⁶ Each bonding state, for example, single bond, double bond, conjugated double bond, and so on, has a specific orbital energy just like fingerprints of molecular vibrations,⁷ and high-energy photons can eject the electrons not only from the highest molecular orbital (HOMO) but also from lower-lying occupied MOs. Therefore, PES using high-energy photons provides us a unique opportunity to gain insight into the molecular structure. This concept is similar to electron spectroscopy for chemical analysis (ESCA), although ESCA probes inner-shell electrons.

Recent development of ultrashort extreme ultraviolet (XUV) pulses by high harmonic generation enables us to access to lower-lying occupied MOs^{8–12} with high temporal resolution from a femtosecond to an attosecond time scale,^{13–18} known as time-resolved PES (TRPES).^{19–21} Although TRPES using visible and ultraviolet lights has been extensively applied to various systems to investigate the ultrafast relaxation processes in the excited states,^{19–21} the ultrafast dynamics of low-lying occupied MOs have rarely been discussed so far. Particular dynamics of each low-lying occupied MO is expected to reveal the temporal evolution of a molecular structure.

In this work, we investigated not only ultrafast relaxation dynamics but also bond-breaking dynamics of 1,2-butadiene by TRPES and ab initio theoretical calculations. Upon ultraviolet excitation at 193 nm, photofragment translational spectroscopy (PTS) has shown that 1,2-butadiene has two dissociation channels, $\text{CH}_3 + \text{C}_3\text{H}_3$ and $\text{C}_4\text{H}_5 + \text{H}$, with a branching ratio of 96:4.²² It has been suggested that these two dissociations take place after the internal conversion to the ground state.²² Thus, we were interested in the ultrafast relaxation processes in 1,2-butadiene, which is a cumulated diene in contrast with 1,3-butadiene,¹² and were motivated to study the relatively simple bond-breaking dynamics by observing the dynamics of lower-lying occupied MOs.

Experimentally, 42 nm (= 29.5 eV) high harmonic pulses were used to probe 1,2-butadiene pumped by two-photon excitation at 400 nm (= 3.1 eV). Because of the lower symmetry, 1,2-butadiene can be excited to the S_1 state in the two-photon process. A time-delay-compensated monochromator (TDCM) was employed to separate the single harmonic (42 nm) with a temporal duration preserved.^{1223–25} The response function of the system was 98 fs, which is limited by the pump pulse duration. (See the Supporting Information for experimental details.) Because 1,2-butadiene is ionized by the photons higher than 9.0 eV,²⁶ which is lower than the three-

Received: May 7, 2015

Accepted: June 11, 2015

photon energy (= 9.3 eV), two-photon absorption was the main excitation process in the present experiment. If the molecules absorbed three photons, they would be ionized and the photoelectron spectrum of the ion should be different largely.

To understand the experimental spectra, the ionization energies were calculated as follows: The geometry optimization was carried out for 1,2-butadiene, propargyl (C_3H_3) radical, and methyl radical in the ground state, by the long-range-corrected density functional theory (LC-DFT)⁶ with LC-BOP/cc-pVDZ using the GAMESS-package.²⁷ For radical species, the spin-unrestricted scheme was employed. The shapes for the α -spin MO are summarized in Figure 1 with the calculated orbital

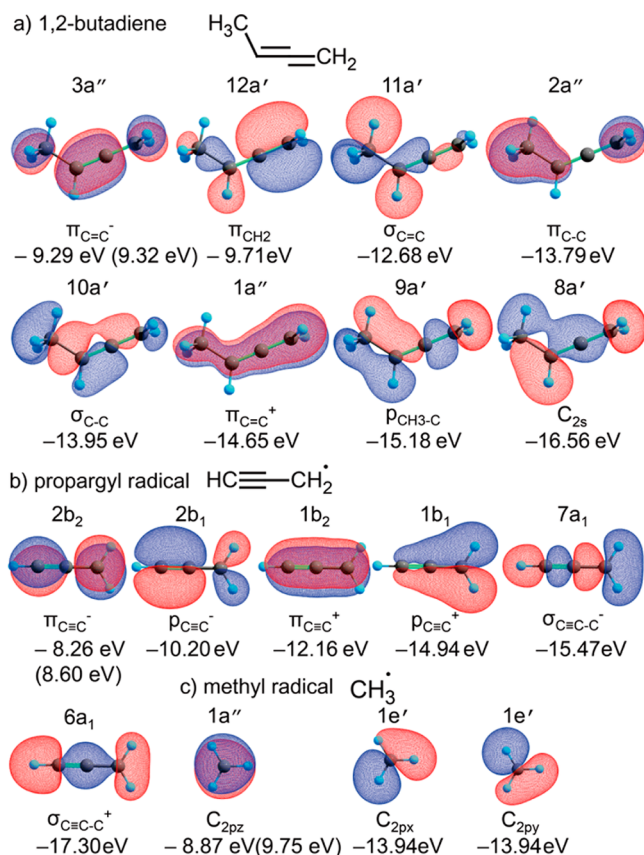


Figure 1. Molecular orbitals and structural formula of (a) 1,2-butadiene, (b) propargyl radical, and (c) methyl radical calculated at the LC-BOP/cc-pVDZ level. The character and orbital energy of each MO are also indicated. The calculated vertical first-ionization energies are shown in the parentheses for HOMOs.

energies and the vertical ionization energies of the HOMO electrons. The ionization energies for the respective molecules were estimated from the orbital energies under Koopmans' theorem, except for the first ionization energies, which were calculated as the vertical ionization energies, that is, energy differences between the neutral and cationic species with the optimized geometry of neutral species. The calculated vertical ionization energies of 1,2-butadiene, propargyl radical, and methyl radical are consistent with the experimental values 9.33,²⁶ 8.67,²⁸ and 9.84 eV,²⁹ respectively.

First, we investigated the relaxation processes to the ground state before the dissociation on the femtosecond time scale. The following two features were found on the femtosecond time scale: (1) Figure 2a shows the 3D plot of the time-resolved photoelectron spectrum. All of the photoelectron

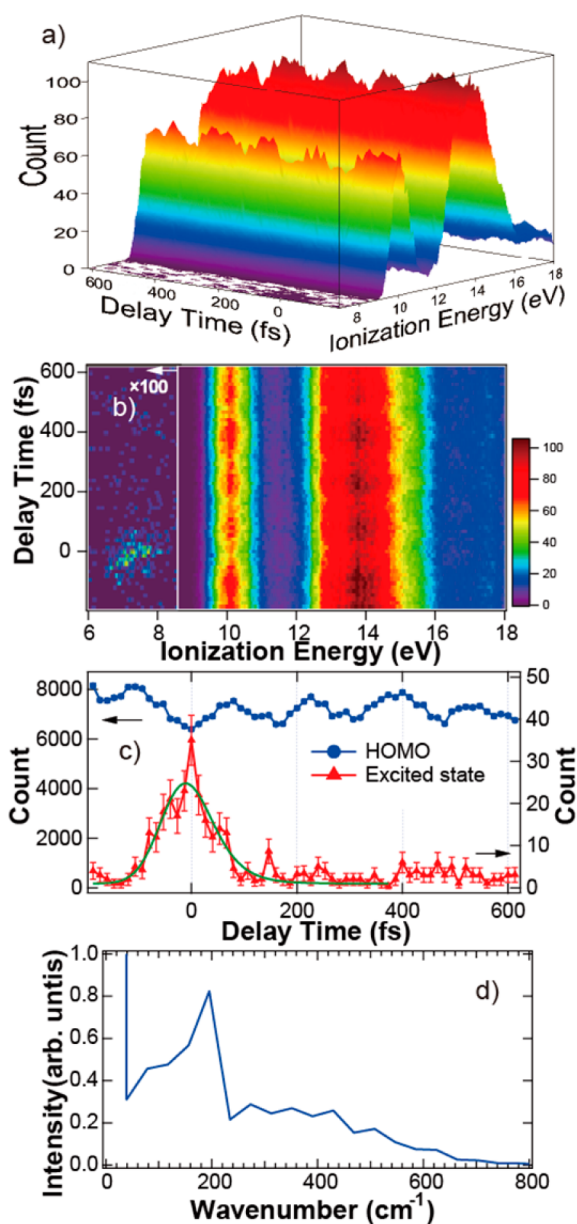


Figure 2. (a) 3D plot of the temporal evolution of the photoelectron spectrum of 1,2-butadiene in the femtosecond region. (b) Photoelectron spectrogram. The color scale indicates the electron count. (c) Time dependence of the photoelectron count of the HOMO band (blue circle) integrated between 9.23 and 11.25 eV and that of the transient excited state (red triangle) integrated between 6.28 and 8.41 eV. The green line is the fitting result to the experimental data. (d) Fourier-transformed spectrum of the HOMO band in panel c.

bands between 7 and 16 eV started oscillating in phase. (2) At 0 fs, a transient photoelectron band was observed at 7.3 eV in the photoelectron spectrogram shown in Figure 2b. Because the energy separation from the HOMO band was 2.8 eV, the transient band was assigned not to the cross correlation between 400 nm (= 3.1 eV) and the 19th harmonic photons by two-photon absorption³⁰ but to an excited state. We did not observe any other transient bands between 2 and 9 eV. Figure 2c shows the time dependence of the integrated HOMO band between 9.23 and 11.25 eV (blue) and the transient excited state integrated between 6.28 and 8.41 eV (red). The lifetime of

the excited state was estimated to be 37 ± 15 fs by least-squares fitting. (See the Supporting Information.)

To clarify the ultrafast relaxation mechanism, the steepest descent pathway was calculated from the Franck–Condon (FC) structure (denoted as $(S_0)_{\min}$) on the S_1 potential energy surface by the multistate multireference perturbation theory (MS-CASPT2) with the basis set of cc-pVDZ using MOLPRO2012,³¹ where two sets of π and π^* orbitals were included in the active space of the reference CASSCF wave function. The three lowest states were solved equally for state-averaged CASSCF, and they were mixed after the perturbation in the MS-CASPT2 calculation. To determine the steepest descent pathway in the excited state, we employed the avoiding model function (AMF) method, with the GRRM11 package.^{32,33} Figure 3a shows the optimized structure of $(S_0)_{\min}$ and

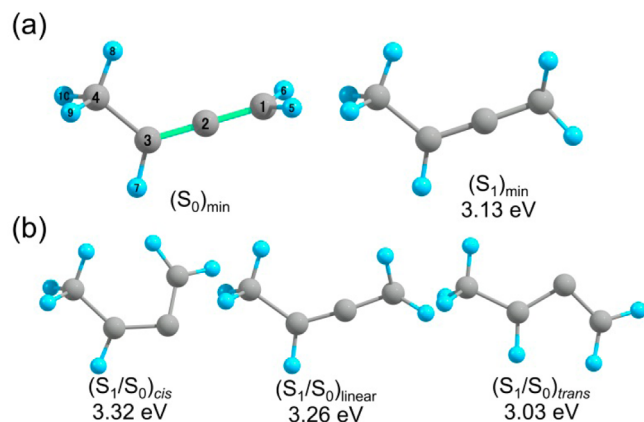


Figure 3. (a) Geometry of 1,2-butadiene at $(S_0)_{\min}$ and $(S_1)_{\min}$ with the numbering of atoms. (b) Three MECI structures, $(S_1/S_0)_{cis}$, $(S_1/S_0)_{linear}$, and $(S_1/S_0)_{trans}$, with the energy relative to $(S_0)_{\min}$.

a terminal of the steepest descent pathway from the FC structure in the S_1 state (denoted as $(S_1)_{\min}$). The numbering of atoms is also shown for $(S_0)_{\min}$. Their geometrical difference indicates that a dominant geometrical change upon photoexcitation of 1,2-butadiene is a rotational motion of the CH_2 fragment at the edge.

To examine dynamical effects on the relaxation pathways, we performed an ab initio molecular dynamics (AIMD) simulation at the MS-CASPT2/cc-pVDZ level by a developmental version of the SPPR program.³⁴ The initial atomic coordinates and velocities were generated by a normal-mode sampling method under a Boltzmann distribution at 300 K in the ground state of 1,2-butadiene, and the trajectories were started upon excitation to the S_1 state. 50 trajectories were calculated until reaching the S_1/S_0 -crossing region, where either the energy difference becomes <0.2 eV or the simulation time reaches up to 0.4 ps. The nonadiabatic transition was not considered in the present simulation. As a result of the AIMD simulations, trajectories can be classified to three types, depending on the terminal regions, that is, cis-like, linear-like, and trans-like structures of the C–C–C framework. The branching ratios for cis-, linear-, and trans-like structures were found to be 2:44:4, and thus, the dominant relaxation pathway after S_1 excitation goes through the linear-like structure.

The minimum energy conical intersections (MECIs) between the S_1 and S_0 states were optimized for the three decay pathways at the MS-CASPT2/cc-pVDZ level by the updated branching plane method.³⁵ Figure 3b shows three

optimized MECI structures. Among the three MECIs, $(S_1/S_0)_{cis}$ was newly found in the present study.³⁶ These results indicate the existence of three decay pathways in the S_1 state of 1,2-butadiene and that the excited 1,2-butadiene quickly reaches $(S_1)_{\min}$ and decays to the ground state via $(S_1/S_0)_{linear}$ in most cases.

Because the AIMD trajectories remain mainly around $(S_1)_{\min}$, we suspect that the experimentally observed transient state shown in Figure 2b comes from $(S_1)_{\min}$. Hence the ionization energy of $(S_1)_{\min}$ was calculated as the energy difference between the neutral and cationic species at the MS-CASPT2/cc-pVDZ level. The ionization energy was calculated to be 6.9 eV for the $(S_1)_{\min}$ structure, which well reproduces the 7.3 eV ionization energy of the transient band obtained by integrating the spectrogram between 100 and -100 fs in Figure 2b. Thus, the transient band is attributed to the photoelectrons from the states around $(S_1)_{\min}$.

Now, we would like to discuss the oscillation of the photoelectron yield from the ground state upon photoexcitation. The vibrational frequency of the HOMO band obtained by Fourier transformation shown in Figure 2d has a peak at 195 cm^{-1} , corresponding to the bending mode of $\text{C}=\text{C}=\text{C}$ in the ground state of 1,2-butadiene predicted by our theoretical calculation and also observed by infrared absorption spectroscopy.³⁷ Therefore, the bending mode of $\text{C}=\text{C}=\text{C}$ was stimulated upon photoexcitation.

The vibrational mode can generate the coherent oscillation of the photoionization probability via FC coupling or Hertzberg–Teller (HT) coupling.^{38,39} The former comes from the quantum beat among the coherently excited vibrational states, and the latter induces the modulation of the transition dipole moment with a frequency of the vibrational mode, known as intensity borrowing.^{38–40} We attribute the mechanism of the oscillation to the HT coupling because the observed phase of the oscillation was constant across the HOMO band including several vibronic states. We evaluated the phases within the HOMO band by slicing the band at 0.3 eV intervals, and each slice has the same phase within $\pm\pi/20$. If the oscillation is induced by the FC coupling, the phase depends on the final vibrational state and is not constant within the HOMO band.²¹ In contrast, the HT coupling stimulates the oscillations with a constant phase within the same electronic state.³⁸

Then, how is that vibrational mode excited? There are two possible mechanisms: one is the impulsive stimulated Raman process for electronically nonexcited molecules and the other is the impulsive absorption of the excited molecules. In the former case, the vibrationally and electronically excited molecules are different, and the observed oscillation is due to the vibrationally excited ones. In the latter case, the dynamical simulation suggests the structural distortion in the excited state, stimulating the bending of $\text{C}=\text{C}=\text{C}$ and the rotation of CH_2 . The observed lifetime of the excited state is shorter than the vibrational period, 171 fs. Hence, the ultrafast excitation and relaxation taking place faster than the vibrational period can stimulate the vibrations. We suspect that the latter is responsible for the observed oscillation because we did not see any oscillations in 1,3-butadiene.¹² If the coherent oscillation was stimulated by the former, the similar oscillation should be observed, suggesting that the stimulated vibrational mode depends on the deformed structure of the molecule in the excited state.

Now, we would like to look into the dissociation dynamics on the picosecond time scale. Figure 4a summarizes the

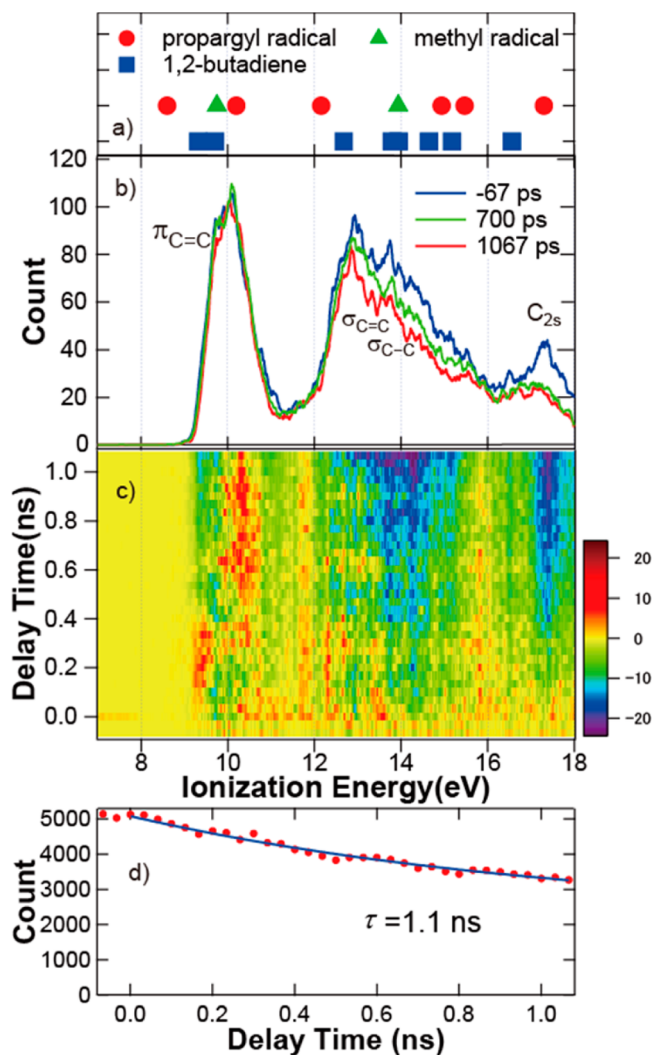


Figure 4. (a) Calculated ionization energies of propargyl (circle) and methyl (triangle) radicals and 1,2-butadiene (square). (b) Time-resolved photoelectron spectra of 1,2-butadiene at -67 (blue), 700 (green), and 1067 (red) ps. (c) Difference photoelectron spectrogram of 1,2-butadiene. The color scale indicates the difference electron count. (d) Time dependence of the intensity of the C_{2s} band integrated between 17.16 and 17.43 eV. The solid line shows the fitting result with a decay time of 1.1 ns.

theoretical ionization energies of 1,2-butadiene, propargyl radicals, and methyl radical listed in Figure 1. Figure 4b,c shows the photoelectron spectra at -67 (blue), 700 (green), and 1067 (red) ps and the difference photoelectron spectrogram from the average spectra of negative delay times, respectively. We found the following four features in Figure 4: (1) The C_{2s} peak at 17.3 eV decreased with time, corresponding to the decreasing area (shown in blue) around 17.3 eV in Figure 4c. (2) Figure 2c,d shows that the band related to the C–C bond between 13.5 and 15.0 eV, consisting of π_{C-C} , σ_{C-C} , and p_{CH_3-C} , also decreased with time, whereas the intensity of the band related to the C=C bond between 12.0 and 13.0 eV, $\sigma_{C=C}$, did not change significantly. (3) In Figure 4d, the area in red shows that the photoelectron yield at 10.3 eV increased after 400 ps. (4) In Figure 4d, the

photoelectron yield at 9.3 eV increased between 100 and 400 ps, indicating the shift of the ionization energy.

Let us discuss the first and second points. A previous study using PTS excited at 193 and 157 nm showed that the dissociation to methyl and propargyl radicals through the bond cleavage of the C–C bond is the dominant process.^{22,41} Therefore, the photoelectron yield from a MO with a large electron density on the C–C bond is expected to decrease. In fact, both the C–C-related band between 13.5 and 15.0 eV and the C_{2s} band were experimentally observed to decrease, which indicates C–C bond cleavage. In addition, the propargyl and methyl radicals appearing after dissociation have fewer MOs around 14 eV, corresponding to σ_{C-C} , as shown in Figure 1. Hence, the photoelectron yield around 14 eV is expected to become smaller by dissociation, and the observed temporal evolution of the photoelectron spectrum is, therefore, equivalent to the real-time observation of dissociation in 1,2-butadiene.

To estimate the dissociation time, we plotted the photoelectron yield of the C_{2s} band between 16.2 and 17.8 eV as a function of time t in Figure 4d. The decay time τ was estimated to be 1.1 ± 0.2 ns by fitting to $A + B \exp(-t/\tau)$, where A and B are constants. The decay rate $1/\tau$ was $0.91 \times 10^9/s$, which is consistent with Rice–Ramsperger–Kassel–Marcus (RRKM)-calculated unimolecular rate of $5.2 \times 10^{10}/s$ upon 193 nm excitation.⁴²

Let us move on to the third finding. PTS has shown that propargyl radicals are formed after dissociation.²² The theoretical calculation shown in Figure 4a predicts that the $p_{C\equiv C}$ orbital energy of propargyl radicals shifts to 10.2 eV and was experimentally found to be 10.3 eV after 400 ps, as shown in Figure 4c. No other bands, however, explicitly appeared in the spectrogram. We suspect that this is due to the spectral broadening by the vibrationally excited states populated by the intramolecular vibrational redistribution (IVR) of the excess energy by photoexcitation. The formation of the vibrationally excited state after dissociation has already been observed in PTS experiment,²² where the photoionization threshold of dissociated propargyl radicals became to be smaller by the population to vibrationally hot states.

The fourth finding is closely related to the third. Upon photoexcitation, the excess energy is distributed among vibrational modes after the relaxation to the ground state. Thus, 1,2-butadiene should also be in the vibrationally hot states before dissociation. Therefore, the increase in the photoelectron yield at 9.3 eV is attributable to the ionization from the vibrationally hot states. This is supported by the time dependence of the photoelectron yield, which decreased after 400 ps in accordance with the appearance of propargyl radical previously discussed. The time dependences of these two bands are shown in the Supporting Information.

Finally, how are the femtosecond and picosecond dynamics correlated? One possible temporal sequence is that the amplitude of the C=C=C bending vibration upon photoexcitation is so large in the femtosecond region that the methyl radical breaks away in the picosecond time scale; however, if the vibrational mode with large amplitude stimulated the dissociation, the molecules should dissociate within several periods of oscillation. However, the observed dissociation time was 1.1 ± 0.2 ns. Therefore, the absorbed excitation energy is redistributed among all vibrational modes through IVR and the dissociation then takes place stochastically.

■ ASSOCIATED CONTENT

■ Supporting Information

Details of experimental methods, experimental setup for time-resolved photoelectrons spectroscopy using high harmonic pulses, cross-correlation function between the pump and the probe pulse, and time dependence of the photoelectron yield on the picosecond timescale. The Supporting Information is available free of charge on the ACS Publications website at DOI: 10.1021/acs.jpcllett.5b00943.

■ AUTHOR INFORMATION

Corresponding Author

*E-mail: sekikawa@eng.hokudai.ac.jp.

Notes

The authors declare no competing financial interest.

■ ACKNOWLEDGMENTS

T.S. was supported by KAKENHI (26600107 and 15H03702) and the Eno Science Foundation. T.T. was supported by KAKENHI (26288001). Part of the calculations was performed on supercomputers at Research Center for Computational Science, Okazaki, Japan.

■ REFERENCES

- (1) Blanchet, V.; Zgierski, M. Z.; Seideman, T.; Stolow, A. Discerning Vibronic Molecular Dynamics Using Time-Resolved Photoelectron Spectroscopy. *Nature* **1999**, *401*, 52–54.
- (2) Lochbrunner, S.; Schultz, T.; Schmitt, M.; Shaffer, J. P.; Zgierski, M. Z.; Stolow, A. Dynamics of Excited-State Proton Transfer Systems Via Time-Resolved Photoelectron Spectroscopy. *J. Chem. Phys.* **2001**, *114*, 2519–2522.
- (3) Satzger, H.; Townsend, D.; Zgierski, M. Z.; Patchkovskii, S.; Ullrich, S.; Stolow, A. Primary Processes Underlying the Photostability of Isolated DNA Bases: Adenine. *Proc. Natl. Acad. Sci. U.S.A.* **2006**, *103*, 10196–10201.
- (4) Sekikawa, T.; Schalk, O.; Wu, G.; Boguslavskiy, A. E.; Stolow, A. Initial Processes of Proton Transfer in Salicylideneaniline Studied by Time-Resolved Photoelectron Spectroscopy. *J. Phys. Chem. A* **2013**, *117*, 2971–2979.
- (5) Schalk, O.; Boguslavskiy, A. E.; Stolow, A. Two-Photon Excited State Dynamics of Dark Valence, Rydberg, and Superexcited States in 1,3-Butadiene. *J. Phys. Chem. Lett.* **2014**, *5*, 560–565.
- (6) Tsuneda, T.; Song, J.-W.; Suzuki, S.; Hirao, K. On Koopmans' Theorem in Density Functional Theory. *J. Chem. Phys.* **2010**, *133*, 174101.
- (7) Kimura, K. *Handbook of HeI Photoelectron Spectra of Fundamental Organic Molecules: Ionization Energies, Ab Initio Assignments, and Valence Electronic Structure for 200 Molecules*; Japan Scientific Societies Press: Tokyo, 1981.
- (8) Nugent-Glandorf, L.; Scheer, M.; Samuels, D. A.; Mulhisen, A. M.; Grant, E. R.; Yang, X.; Bierbaum, V. M.; Leone, S. R. Ultrafast Time-Resolved Soft X-Ray Photoelectron Spectroscopy of Dissociating Br₂. *Phys. Rev. Lett.* **2001**, *87*, 193002.
- (9) Wernet, P.; Odellius, M.; Godehusen, K.; Gaudin, J.; Schwarzkopf, O.; Eberhardt, W. Real-Time Evolution of the Valence Electronic Structure in a Dissociating Molecule. *Phys. Rev. Lett.* **2009**, *103*, 013001.
- (10) Wernet, P. Electronic Structure in Real Time: Mapping Valence Electron Rearrangements During Chemical Reactions. *Phys. Chem. Chem. Phys.* **2011**, *13*, 16941–16954.
- (11) Fushitani, M.; Matsuda, A.; Hishikawa, A. Time-Resolved Evv Photoelectron Spectroscopy of Dissociating I₂ by Laser Harmonics at 80 Nm. *Opt. Express* **2011**, *19*, 9600–9606.
- (12) Makida, A.; Igarashi, H.; Fujiwara, T.; Sekikawa, T.; Harabuchi, Y.; Taketsugu, T. Ultrafast Relaxation Dynamics in Trans-1,3-Butadiene Studied by Time-Resolved Photoelectron Spectroscopy with High Harmonic Pulses. *J. Phys. Chem. Lett.* **2014**, *5*, 1760–1765.
- (13) Hentschel, M.; Kienberger, R.; Spielmann, C.; Reider, G. A.; Milosevic, N.; Brabec, T.; Corkum, P.; Heinzmann, U.; Drescher, M.; Krausz, F. Attosecond Metrology. *Nature* **2001**, *414*, 509–513.
- (14) Sekikawa, T.; Kosuge, A.; Kanai, T.; Watanabe, S. Nonlinear Optics in the Extreme Ultraviolet. *Nature* **2004**, *432*, 605–608.
- (15) Goulielmakis, E.; Schultze, M.; Hofstetter, M.; Yakovlev, V. S.; Gagnon, J.; Uiberacker, M.; Aquila, A. L.; Gullikson, E. M.; Attwood, D. T.; Kienberger, R.; Krausz, F.; Kleineberg, U. Single-Cycle Nonlinear Optics. *Science* **2008**, *320*, 1614–1617.
- (16) Zhao, K.; Zhang, Q.; Chini, M.; Wu, Y.; Wang, X.; Chang, Z. Tailoring a 67 Attosecond Pulse through Advantageous Phase-Mismatch. *Opt. Lett.* **2012**, *37*, 3891–3893.
- (17) Belshaw, L.; Calegari, F.; Duffy, M. J.; Trabattini, A.; Poletto, L.; Nisoli, M.; Greenwood, J. B. Observation of Ultrafast Charge Migration in an Amino Acid. *J. Phys. Chem. Lett.* **2012**, *3*, 3751–3754.
- (18) Takahashi, E. J.; Lan, P.; Mücke, O. D.; Nabekawa, Y.; Midorikawa, K. Attosecond Nonlinear Optics Using Gigawatt-Scale Isolated Attosecond Pulses. *Nature Commun.* **2013**, *4*, 2691.
- (19) Stolow, A.; Underwood, J. G. Time-Resolved Photoelectron Spectroscopy. *Adv. Chem. Phys.* **2008**, *139*, 497–583.
- (20) Suzuki, Y.-I.; Fuji, T.; Horio, T.; Suzuki, T. Time-Resolved Photoelectron Imaging of Ultrafast S₂->S₁ Internal Conversion through Conical Intersection in Pyrazine. *J. Chem. Phys.* **2010**, *132*, 174302.
- (21) Wu, G.; Hockett, P.; Stolow, A. Time-Resolved Photoelectron Spectroscopy: From Wavepackets to Observables. *Phys. Chem. Chem. Phys.* **2011**, *13*, 18447–18467.
- (22) Robinson, J. C.; Sun, W.; Harris, S. A.; Qi, F.; Neumark, D. M. Photofragment Translational Spectroscopy of 1,2-Butadiene at 193 nm. *J. Chem. Phys.* **2001**, *115*, 8359–8360.
- (23) Ito, M.; Kataoka, Y.; Okamoto, T.; Yamashita, M.; Sekikawa, T. Spatiotemporal Characterization of Single-Order High Harmonic Pulses from Time-Compensated Toroidal-Grating Monochromator. *Opt. Express* **2010**, *18*, 6071–6078.
- (24) Igarashi, H.; Makida, A.; Ito, M.; Sekikawa, T. Pulse Compression of Phase-Matched High Harmonic Pulses from a Time-Delay Compensated Monochromator. *Opt. Express* **2012**, *20*, 3725–3732.
- (25) Igarashi, H.; Makida, A.; Sekikawa, T. Electron Trajectory Selection for High Harmonic Generation inside a Short Hollow Fiber. *Opt. Express* **2013**, *21*, 20632–20640.
- (26) Brogli, F.; Crandall, J. K.; Heilbronner, E.; Kloster-Jensen, E.; Sojka, S. A. The Photoelectron Spectra of Methyl-Substituted Allenes and of Tetramethyl-Bisallenyl. *J. Electron Spectrosc. Relat. Phenom.* **1973**, *2*, 455–465.
- (27) Gordon, M. S.; Schmidt, M. W. Advances in Electronic Structure Theory: Gamess a Decade Later. In *Theory and Applications of Computational Chemistry, The First Forty Years*, Dykstra, C. E., Frenking, G., Kim, K. S., Scuseria, G. E., Eds.; Elsevier: Amsterdam, 2005; pp 1167–1189.
- (28) Gilbert, T.; Pfab, R.; Fischer, I.; Chen, P. The Zero Kinetic Energy Photoelectron Spectrum of the Propargyl Radical, C₃H₃. *J. Chem. Phys.* **2000**, *112*, 2575.
- (29) Houle, F. A.; Beauchamp, J. L. Photoelectron Spectroscopy of Methyl, Ethyl, Isopropyl, and Tert-Butyl Radicals. Implications for the Thermochemistry and Structures of the Radicals and Their Corresponding Carbonium Ions. *J. Am. Chem. Soc.* **1979**, *101*, 4067–4074.
- (30) Sekikawa, T.; Kanai, T.; Watanabe, S. Frequency-Resolved Optical Gating of Femtosecond Pulses in the Extreme Ultraviolet. *Phys. Rev. Lett.* **2003**, *91*, 103902.
- (31) Werner, H.-J.; Knowles, P. J.; Knizia, G.; Manby, F. R.; Schütz, M.; Celani, P.; Korona, T.; Lindh, R.; Mitrushenkov, A.; Rauhut, G.; Shamasundar, K. R.; Adler, T. B.; Amos, R. D.; Bernhardsson, A.; Berning, A.; Cooper, D. L.; Deegan, M. J. O.; Dobbyn, A. J.; Eckert, F.; Goll, E.; Hampel, C.; Hesselmann, A.; Hetzer, G.; Hrenar, T.; Jansen, G.; Köppl, C.; Liu, Y.; Lloyd, A. W.; Mata, R. A.; May, A. J.

McNicholas, S. J.; Meyer, W.; Mura, M. E.; Nicklass, A.; O'Neill, D. P.; Palmieri, P.; Peng, D.; Pflüger, K.; Pitzer, R.; Reiher, M.; Shiozaki, T.; Stoll, H.; Stone, A. J.; Tarroni, R.; Thorsteinsson, T.; Wang, M. *MOLPRO*, version 2012.1, a Package of Ab Initio Programs, <http://www.molpro.net>.

(32) Maeda, S.; Osada, Y.; Morokuma, K.; Ohno, K. *GRRM11*, version 11.01, 2011.

(33) Maeda, S.; Ohno, K.; Morokuma, K. Exploring Multiple Potential Energy Surfaces: Photochemistry of Small Carbonyl Compounds. *Adv. Phys. Chem.* **2012**, *2012*, 268124.

(34) Harabuchi, Y.; Ono, Y.; Okai, M.; Yamamoto, R.; Taketsugu, T. *Developmental Version of SPPR*, 2014.

(35) Maeda, S.; Ohno, K.; Morokuma, K. Updated Branching Plane for Finding Conical Intersections without Coupling Derivative Vectors. *J. Chem. Theory Comput.* **2010**, *6*, 1538–1545.

(36) Maeda, S.; Harabuchi, Y.; Taketsugu, T.; Morokuma, K. Systematic Exploration of Minimum Energy Conical Intersection Structures near the Franck–Condon Region. *J. Phys. Chem. A* **2014**, *118*, 12050–12058.

(37) Bell, S.; Guirgis, G. A.; Durig, J. R. Torsional Transitions and Barrier to Internal Rotation of 1,2-Butadiene. *Spectrochim. Acta* **1989**, *45A*, 479–485.

(38) Ishii, K.; Takeuchi, S.; Tahara, T. Pronounced Non-Condon Effect as the Origin of the Quantum Beat Observed in the Time-Resolved Absorption Signal from Excited-State Cis-Stilbene. *J. Phys. Chem. A* **2008**, *112*, 2219–2227.

(39) Kano, H.; Saito, T.; Kobayashi, T. Observation of Herzberg–Teller-Type Wave Packet Motion in Porphyrin J-Aggregates Studied by Sub-5-Fs Spectroscopy. *J. Phys. Chem. A* **2002**, *106*, 3445–3453.

(40) Atkins, P.; Friedman, R. *Molecular Quantum Mechanics*, 4th ed.; Oxford University Press: Oxford, U.K., 2005.

(41) Mu, X.; Lu, I.-C.; Lee, S.-H.; Wang, X.; Yang, X. Photodissociation Dynamics of 1,2-Butadiene at 157 nm. *J. Chem. Phys.* **2004**, *121*, 4684–4690.

(42) Lee, H.-Y.; Kislov, V.; Lin, S.-H.; Mebel, A. M.; Neumark, D. M. An Ab Initio/RRKM Study of Product Branching Ratios in the Photodissociation of Buta-1,2- and -1,3-dienes and But-2-yne at 193 nm. *Chem.—Eur. J.* **2003**, *9*, 726–740.